Title
On contact point motion in the vibration analysis of elastic rods

Authors
Goldberg, Nathaniel N
O'Reilly, Oliver M

Publication Date
2020-11-01

DOI
10.1016/j.jsv.2020.115579

Peer reviewed

On Contact Point Motion in the Vibration Analysis of Elastic Rods*

Nathaniel N. Goldberg[1], Oliver M. O'Reilly[1]

[a]*Department of Mechanical Engineering, University of California, Berkeley, CA 94720-1740, USA*

Abstract

We present a systematic method for analyzing the vibrations of elastic rods whose effective length is variable, with particular emphasis on rods in unilateral contact with rigid surfaces. Problems of this type abound in engineering applications at all length scales, from the laying of submarine pipelines to the stiction of cantilevers in microelectromechanical systems (MEMS). By a careful treatment of boundary conditions, we elucidate the circumstances under which a rod of variable length can be treated as one of fixed length for the sake of analyzing small-amplitude vibrations. In applying our method to a simple free vibration problem, we encounter an unusual singular limit and observe a close connection between vibration, stability, and existence.

Keywords: rod, beam, variable-length, variable-arc-length, linear vibration, contact, small-on-large

1. Introduction

In studying the mechanics of elastic rods, one occasionally encounters problems in which the effective length of the rod is unknown *a priori*. Such problems are sometimes referred to as "variable-length" or "variable-arc-length" problems among rod mechanicians,[1] a simple example being the lifting of a heavy strip of paper from a table by an upward force applied to one end. Here the effective length is the length of the portion that is not in contact with the table. For a given upward force, this length (and hence the mathematical domain) is not immediately known and must instead be found as part of the solution. The formation of troublesome rucks in rugs and the nesting of rubber bands are other examples involving variable-length rods [4, 5].

Problems of the aforementioned type belong to the class of free boundary-value problems in mathematics. Because one cannot simply add functions defined on dis-

*The authors gratefully acknowledge financial support from the United States Department of Defense through the National Defense Science and Engineering Science Fellowship awarded to N. N. Goldberg.

*Corresponding author

[1]The terms "variable-length" and "variable-arc-length" are sometimes used to refer to problems in which the rod's length varies as a prescribed function of time [1, 2], for example the ejection of paper from a photocopier [3]. However, we use these terms exclusively to refer to problems in which the length is variable *and also initially unknown*.

parate domains, free boundary problems are inherently nonlinear and can produce nonlinear effects even if the underlying differential equations are linear. Furthermore, their solution requires the specification of more boundary conditions than their standard counterparts do. This is apparent in the case of the Euler-Bernoulli beam: a fixed-length beam needs four boundary conditions while a variable-length beam needs five.

It is a largely straightforward numerical computation to solve for the static configuration of a variable-length rod [6], and closed-form analytical solutions are typically available for the small-amplitude regime [7]. There is less understanding, however, on how to appropriately treat small-amplitude vibrations about a statically deformed configuration (both the "small-on-small" and "small-on-large" analyses), even though this task is well-understood for rods of fixed length [8].

A more fundamental insight into the vibration of variable-length rods is certainly of interest from a theoretical point-of-view, but it is also relevant to several vibration-critical engineering applications. Submarine pipelines, flexible risers, and other marine structures that touch the seafloor are essentially variable-length rods [9, 10], as are micro-scale cantilever beams when they adhere electrostatically to the substrate of microelectromechanical systems (MEMS) [11]. Belt-driven transmissions at high speeds and/or with considerable slack can also be effectively modeled as variable-length (and axially translating) rods [12].

The principal difficulty in analyzing the vibrations of variable-length rods is readily illustrated in unilateral contact problems, such as the one illustrated in Fig. 1, in which the contact point moves left and right over the course of the vibratory motion. Some authors argue heuristically that the oscillations of this point are "small" in some sense relative to the overall amplitude of vibrations and proceed to treat the point as being fixed [13, 14]. Others apply variable transformations to map the free boundary to a fixed one [9, 11, 15], while others yet apply perturbation methods to the boundary conditions [10, 16, 17].

The goal of this paper is to clarify the third approach, use it to explain when the first is applicable, and highlight why the second is an unnecessary complication if only linear vibrations are considered. We do all this in the context of the foregoing contact problem, but the technique we outline can be readily applied to a number of other situations involving variable-length rods, such as a roller support or sleeve constraint [18, 19]. Over the course of our analysis, which we present in considerable detail, we explain several counter-intuitive results from the literature. We conclude by providing a thorough numerical exploration of the parameter space for the problem depicted in Fig. 1. A video animating the first three vibration modes is included in the Supplementary Material for this article.

2. Small-Amplitude Vibrations Superposed on Small-Amplitude Equilibria

We now study small-amplitude free vibrations about small-amplitude static equilibria of the system illustrated in Fig. 1, which was first introduced by Roy and Chatterjee [11] and is closely related to a system considered earlier by Demeio and Lenci [9]. In this section we treat the rod as an Euler-Bernoulli beam of linear density ρ_0 and flexural rigidity EI. It is clamped on its left end at a height a from a frictionless, adhesion-free horizontal substrate and is subjected to a downward gravitational force per unit length

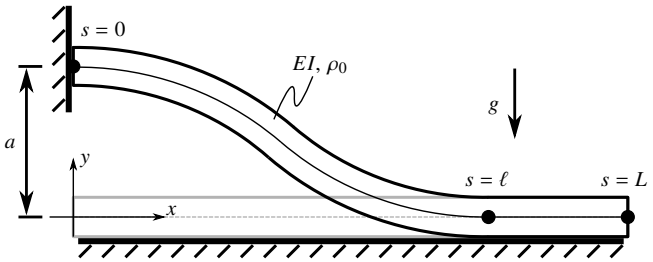

Figure 1: Schematic of the problem first considered by Roy and Chatterjee [11].

of magnitude $\rho_0 g$. The length $\ell = \ell(t)$ of the non-contacting segment of the beam is unknown *a priori* and must be determined as part of the solution. Under static conditions, the non-contacting length is denoted ℓ_0. The total length of the beam is L, which must be greater than $\ell(t)$ for physically meaningful solutions to exist.

As is usual with Euler-Bernoulli beams, it is permissible to exchange the arc-length coordinate s with the abscissa x, making $y = y(x,t)$ and $\ell = \ell(t)$ the sole dependent variables. The dynamics are governed by the familiar equation

$$\rho_0 \frac{\partial^2 y}{\partial t^2} + EI \frac{\partial^4 y}{\partial x^4} + \rho_0 g = 0\,, \quad 0 < x < \ell(t)\,, \quad t > 0\,. \tag{1}$$

We now nondimensionalize Eq. (1). Scaling all lengths by a, scaling time t by $a^2\sqrt{\rho_0/EI}$, and defining $w = \rho_0 g a^3/EI$, we have

$$\frac{\partial^2 y}{\partial t^2} + \frac{\partial^4 y}{\partial x^4} + w = 0\,, \quad 0 < x < \ell(t)\,, \quad t > 0\,. \tag{2}$$

We will work in dimensionless terms for the remainder of the paper. Equation (2) is to be solved subject to the boundary conditions

$$y(0,t) = 1\,, \quad \frac{\partial y}{\partial x}(0,t) = 0\,, \tag{3}$$

and

$$y(\ell(t),t) = 0\,, \quad \frac{\partial y}{\partial x}(\ell(t),t) = 0\,, \quad \frac{\partial^2 y}{\partial x^2}(\ell(t),t) = 0\,. \tag{4}$$

Equation $(4)_3$ is a consequence of the lack of adhesion between the beam and the substrate. (If reversible adhesion were present, the right-hand side would be replaced by a constant $M_\ell > 0$ related to the adhesive energy between the beam and the substrate [20, 21].) Notice that five boundary conditions are required rather than the usual four because $\ell(t)$ is an additional unknown.

We briefly mention that the solution to the right of $x = \ell(t)$ is trivial and need not be given special consideration in the case of an Euler-Bernoulli beam, though this issue must be revisited in the nonlinear regime. Finally, we note that our interest is entirely in steady, oscillatory solutions so we do not specify initial conditions.

2.1. Solution via Variable Transformation

The essence of the method used by Roy and Chatterjee [11] to analyze oscillatory solutions of Eqs. (2) to (4), first introduced by Demeio and Lenci [9] in a slightly different context, is to perform a change-of-variable that maps $x \in (0, \ell(t))$ to a fixed interval, namely $z = x/\ell(t) \in (0, 1)$. Such a transformation changes the free boundary-value problem into a standard boundary-value problem with the additional unknown $\ell(t)$ pushed into the differential equation itself. It also induces the interesting concept of an "extended" mode shape of a vibrating system that contains different material points at different instants in time.

However, the transformation comes at the cost of increased algebraic complexity, as is evident in the resulting expression for the acceleration operator. Writing $y(x, t) = y(\ell(t)z, t) =: \tilde{y}(z, t)$, it can be shown that Eq. (2) becomes

$$\frac{\partial^2 \tilde{y}}{\partial t^2} + \left(\frac{2\dot{\ell}^2}{\ell} - \ddot{\ell}\right)\frac{z}{\ell}\frac{\partial \tilde{y}}{\partial z} - \frac{2\dot{\ell}z}{\ell}\frac{\partial^2 \tilde{y}}{\partial t \partial z} + \left(\frac{\dot{\ell}z}{\ell}\right)^2 \frac{\partial^2 \tilde{y}}{\partial z^2} + \frac{1}{\ell^4}\frac{\partial^4 \tilde{y}}{\partial z^4} + w = 0\,, \tag{5}$$

where $0 < z < 1$ and $t > 0$. The increased complexity apparent in Eq. (5) does not make analysis impossible, but it does obscure some critical facets of the problem. An extensive calculation shows that the natural frequencies ω of small free vibrations about a static solution of Eq. (5), subject to the appropriate boundary conditions in the z-domain derived from Eqs. (3) and (4), are governed by

$$\cos(\sqrt{\omega}\ell_0)\cosh(\sqrt{\omega}\ell_0) - 1 = 0\,. \tag{6}$$

After unraveling the nondimensionalization, it becomes evident that Eq. (6) is *exactly* the same as the characteristic equation for the natural frequencies of a fixed-fixed beam with length equal to the static non-contacting length ℓ_0. This unexpected correspondence, first recognized by Roy and Chatterjee [11], seems nothing less than miraculous from the perspective of the preceding procedure. In the sequel, we demonstrate that the same result follows transparently from an alternative approach that also elucidates the conditions under which similarly unexpected correspondences may exist.

2.2. Solution via Regular Perturbation Expansion

Rather than transform the domain to one of a fixed length, we now elect to work directly with the original statement of the problem in the x-domain, Eqs. (2) to (4). To begin, we expand $y(x, t)$ and $\ell(t)$ in regular perturbation series:

$$y(x, t) = y_0(x) + \epsilon y_1(x, t) + O(\epsilon^2)\,, \quad \ell(t) = \ell_0 + \epsilon\ell_1(t) + O(\epsilon^2)\,. \tag{7}$$

We will truncate these series to $O(\epsilon)$ in order to obtain the leading-order dynamics about the static equilibrium. Inserting Eq. $(7)_1$ into Eq. (2) and grouping powers of ϵ, we find

$$\frac{d^4 y_0}{dx^4} + w = 0\,, \quad \frac{\partial^2 y_1}{\partial t^2} + \frac{\partial^4 y_1}{\partial x^4} = 0\,. \tag{8}$$

Equation (3) then implies the following boundary conditions at $x = 0$:

$$y_0(0) = 1\,, \quad y_1(0, t) = 0\,, \quad \frac{dy_0}{dx}(0) = 0\,, \quad \frac{\partial y_1}{\partial x}(0, t) = 0\,. \tag{9}$$

It is slightly more complicated to determine the consequences of the perturbation expansion for Eq. (4), the boundary conditions at the free boundary $x = \ell(t)$. Starting with Eq. $(4)_3$ and neglecting terms quadratic or higher in ϵ,

$$\begin{aligned} 0 &= \frac{\partial^2 y}{\partial x^2}(\ell(t), t) \\ &= \frac{\partial^2 y}{\partial x^2}(\ell_0 + \epsilon \ell_1(t), t) \\ &= \frac{d^2 y_0}{dx^2}(\ell_0 + \epsilon \ell_1(t)) + \epsilon \frac{\partial^2 y_1}{\partial x^2}(\ell_0 + \epsilon \ell_1(t), t) \\ &= \frac{d^2 y_0}{dx^2}(\ell_0) + \epsilon \left[\frac{d^3 y_0}{dx^3}(\ell_0)\ell_1(t) + \frac{\partial^2 y_1}{\partial x^2}(\ell_0, t) \right], \end{aligned} \tag{10}$$

which immediately yields

$$\frac{d^2 y_0}{dx^2}(\ell_0) = 0\,, \quad \frac{d^3 y_0}{dx^3}(\ell_0)\ell_1(t) + \frac{\partial^2 y_1}{\partial x^2}(\ell_0, t) = 0\,. \tag{11}$$

Carefully applying the same procedure to Eq. $(4)_2$, we obtain

$$\frac{dy_0}{dx}(\ell_0) = 0\,, \quad \underbrace{\frac{d^2 y_0}{dx^2}(\ell_0)}_{=0 \text{ by Eq. } (11)_1} \ell_1(t) + \frac{\partial y_1}{\partial x}(\ell_0, t) = 0\,. \tag{12}$$

Finally, we obtain from Eq. $(4)_1$,

$$y_0(\ell_0) = 0\,, \quad \underbrace{\frac{dy_0}{dx}(\ell_0)}_{=0 \text{ by Eq. } (12)_1} \ell_1(t) + y_1(\ell_0, t) = 0\,. \tag{13}$$

To summarize, we have the following straightforward-to-solve free boundary-value problem for the static equilibrium:

$$\frac{d^4 y_0}{dx^4} + w = 0\,, \tag{14}$$

$$y_0(0) = 1\,, \tag{15}$$

$$\frac{dy_0}{dx}(0) = 0\,, \tag{16}$$

$$y_0(\ell_0) = 0\,, \tag{17}$$

$$\frac{dy_0}{dx}(\ell_0) = 0\,, \tag{18}$$

$$\frac{d^2 y_0}{dx^2}(\ell_0) = 0\,, \tag{19}$$

which has the solution

$$y_0(x) = \left(1 - \frac{x}{\ell_0}\right)^3 \left(1 + \frac{3x}{\ell_0}\right), \quad \ell_0 = \left(\frac{72}{w}\right)^{1/4}. \tag{20}$$

Additionally, $y_1(x,t)$ is governed by

$$\frac{\partial^2 y_1}{\partial t^2} + \frac{\partial^4 y_1}{\partial x^4} = 0\,, \tag{21}$$

$$y_1(0,t) = 0\,, \tag{22}$$

$$\frac{\partial y_1}{\partial x}(0,t) = 0\,, \tag{23}$$

$$y_1(\ell_0,t) = 0\,, \tag{24}$$

$$\frac{\partial y_1}{\partial x}(\ell_0,t) = 0\,. \tag{25}$$

Finally, $\ell_1(t)$ is determined from the sole remaining piece of information derived from the original boundary conditions, Eq. $(11)_2$.

Equations (21) *to* (25) *are precisely the equations governing the dynamics of a fixed-fixed beam of length* ℓ_0*!* This transparently shows the same result obtained in Section 2.1 by way of a clever but substantially more involved computation. In fact, our result is somewhat more general: it is not just the natural frequencies that are the same as those for a fixed-fixed beam of appropriate length, but rather the *entire first-order dynamics*. The present method also illustrates the interesting fact that *the dynamical effect of the motion of the contact point is negligible to first order and hence the concept of an "extended" mode shape as introduced in Section 2.1 is superfluous*. Lastly, it is interesting to observe that the neither the static solution, Eq. (20), nor the dynamics defined by Eqs. (21) to (25) depend on the specific weight w except through ℓ_0.

2.3. Solution to a Modified Problem

Roy and Chatterjee also consider an alternate problem without gravity but with an adhesive substrate [11]. They find that the equation for the natural frequencies in this case does *not* correspond to any well-known formula. Our method makes it easy to see why this is the case. We will consider the combined effect of gravity and adhesion, but the results readily degenerate to the adhesion-only case.

When adhesion is present, Eq. $(4)_3$ is replaced by

$$\frac{\partial^2 y}{\partial x^2}(\ell(t),t) = M_\ell\,, \tag{26}$$

where $M_\ell > 0$ is a specified constant related to the adhesion energy between the rod and the substrate [20, 21]. Equation $(11)_1$ is then replaced by

$$\frac{d^2 y_0}{dx^2}(\ell_0) = M_\ell\,, \tag{27}$$

whence Eq. $(12)_2$ becomes

$$M_\ell \ell_1(t) + \frac{\partial y_1}{\partial x}(\ell_0,t) = 0\,, \tag{28}$$

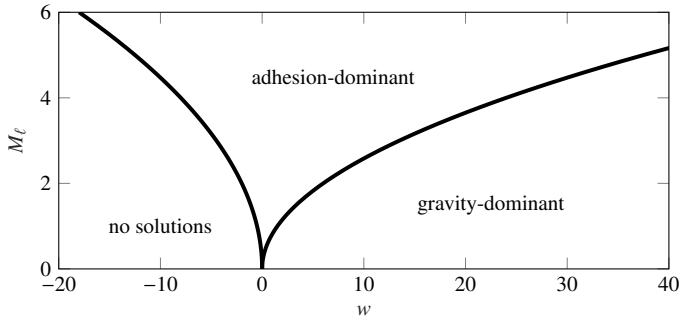

Figure 2: Classification of solutions to the static problem in terms of the parameters w and M_ℓ, according to the linear (Euler-Bernoulli) analysis.

or, upon combination with Eq. $(11)_2$,

$$\underbrace{\frac{\partial^2 y_1}{\partial x^2}(\ell_0,t)}_{\text{bending moment}} = K \underbrace{\frac{\partial y_1}{\partial x}(\ell_0,t)}_{\text{rotation angle}}, \quad K = \frac{1}{M_\ell}\frac{d^3 y_0}{dx^3}(\ell_0)\,. \tag{29}$$

Notice that Eq. (29) is equivalent to a rotational spring at the boundary $x = \ell_0$ with (dimensionless) stiffness K, which in general depends on the constant M_ℓ that characterizes adhesion as well as the static configuration $\{y_0(x), \ell_0\}$. Omitting some minor details, said configuration can be shown to be governed by Eqs. (14) to (18) and Eq. (27). The solution is

$$y_0(x) = (\ell_0 - x)^2\left[\frac{1}{2}M_\ell + \frac{1}{6}\left(\frac{1}{3}w\ell_0 - \frac{2}{\ell_0}M_\ell\right)(\ell_0 - x) - \frac{1}{24}w(\ell_0 - x)^2\right], \tag{30}$$

where the non-contacting length ℓ_0 is such that is satisfies

$$w\ell_0^4 + 12M_\ell\ell_0^2 - 72 = 0\,. \tag{31}$$

Equation (31) is quadratic in ℓ_0^2 and hence physically meaningful solutions exist only if the discriminant is non-negative, which implies the simple constraint $M_\ell^2 + 2w \geq 0$. The system can therefore only access a certain region of the (w, M_ℓ)-plane.

Where solutions do exist, it is instructive to classify them into two types. We call a solution *gravity-dominant* if the vertical force between the beam and the substrate at $x = \ell_0$ is compressive. If said force is tensile, we call the solution *adhesion-dominant*. The boundary between these two regions in the (w, M_ℓ)-plane is characterized by zero vertical force at $x = \ell_0$. It can be shown using Eq. (30) and Eq. (31) that points on the boundary satisfy $2w = 3M_\ell^2$. Figure 2 is a graphical classification of the static equilibria in the parameter space.

The first-order dynamics[2] in the case of combined gravity and adhesion are governed by Eqs. (21) to (24) and Eq. (29), except with the rotational spring stiffness K

[2]Notice that when $w = 0$ the dynamics depend on M_ℓ only through ℓ_0, just as the dynamics depend on w only through ℓ_0 when $M_\ell = 0$.

given according to

$$K = \frac{1}{M_\ell}\frac{d^3 y_0}{dx^3}(\ell_0) = \frac{2}{\ell_0} - \frac{w\ell_0}{3M_\ell}\,. \tag{32}$$

Such a set of equations of course describe a beam fixed at $x = 0$ and restrained by a rotational spring at $x = \ell_0$. This specific combination of boundary conditions does not constitute a standard case and hence it is natural that Roy and Chatterjee [11] did not recognize the correspondence from the characteristic equation for the natural frequencies of free vibration. It is a mostly elementary exercise to solve for the natural frequencies and we report the procedure in Appendix A; when $w = 0$ the results agree with Roy and Chatterjee's.[3]

3. Small-Amplitude Vibrations Superposed on Large-Amplitude Equilibria

Understanding now the general procedure by which one can analyze small-amplitude vibrations of variable-length Euler-Bernoulli beams about small-amplitude static configurations, it is not a particularly challenging task to pass through to the small-on-large regime for an inextensible, unshearable, planar *elastica* of variable length. In this section and the next we again specialize our results to the problem considered in the linear context in Section 2, including the effects of both gravity and adhesion, but the procedure by which one would solve a more general class of problems should be evident.

3.1. General Solution Procedure

Following notation similar to that used elsewhere [8, 13, 22], the dimensionless governing equations can be expressed in slightly modified form as

$$\frac{\partial F}{\partial s} = \frac{\partial^2 x}{\partial t^2}\,, \tag{33}$$

$$\frac{\partial G}{\partial s} = \frac{\partial^2 y}{\partial t^2} + w\,, \tag{34}$$

$$\frac{\partial m}{\partial s} = F\sin\theta - G\cos\theta\,, \tag{35}$$

$$\frac{\partial \theta}{\partial s} = m\,, \tag{36}$$

$$\frac{\partial x}{\partial s} = \cos\theta\,, \tag{37}$$

$$\frac{\partial y}{\partial s} = \sin\theta\,, \tag{38}$$

all of which hold for $0 < s < \ell(t)$ and $t > 0$. All lengths have been scaled by a, the forces F and G by EI/a^2, the bending moment m by EI/a, and time t by $a^2\sqrt{\rho_0/EI}$. As in Section 3.1, $w = \rho_0 g a^3/EI$.

[3] Roy and Chatterjee [11] use a different nondimensionalization than we do. Their angular natural frequencies are numerically equivalent to our $\omega\ell_0^2$.

Equations (33) and (34) are the horizontal and vertical components of the balance of linear momentum, respectively, while Eq. (35) is the balance of angular momentum, neglecting rotary inertia. Equation (36) is the moment-curvature constitutive law. Finally, Eqs. (37) and (38) are collectively the definition of the angle θ. Equations (33) to (38) require seven total boundary conditions rather than the usual six, as $\ell(t)$ is an additional unknown.

Our derivation follows a recipe only incrementally more complex than that employed in Section 2.2. It is as follows:

- Assume that each of the seven dependent variables—F, G, m, θ, x, y, and ℓ—can be written as a static term plus a small dynamic term, e.g., $m(s,t) = m_0(s) + \epsilon m_1(s,t)$, $\epsilon \ll 1$.

- Plug the aforementioned *Ansätze* into Eqs. (33) to (38) and expand terms in Taylor series as needed to isolate the coefficients of ϵ^0 and ϵ^1. The former yield the differential equations governing the static terms (e.g., $m_0(s)$), while the latter yield those governing the dynamic terms (e.g., $m_1(s,t)$), which will depend parametrically on the static solution.

- Plug the *Ansätze* into the boundary conditions and again expand in Taylor series as needed to isolate a hierarchy of boundary conditions, paying special attention to the conditions at $s = \ell(t)$. Seven boundary conditions for the static variables will result as well as seven for the dynamic variables. However, the latter can be combined in such a way so as to produce just six conditions (the total number needed to specify the solution for the dynamic problem on the fixed interval $0 < s < \ell_0$), as well as an equation for $\ell_1(t)$ in terms of the static and dynamic solutions.

- Assume that each dynamic term (except for $\ell_1(t)$) is the product of a function of s and a sinusoid, e.g., $m_1(s,t) = \hat{m}_1(s)\cos(\omega t)$. The collection of the "hatted" functions constitutes the mode shape of the rod and ω is the natural frequency that must be determined as part of the solution.

- Obtain boundary conditions for the mode shapes from the boundary conditions for the dynamic variables.

This procedure is in fact quite general and can be applied to a range of problems.

3.2. Perturbation Expansion of Governing Equations

We now explicitly apply the small-on-large analysis procedure introduced in Section 3.1 to the familiar example illustrated in Fig. 1, and for which Eqs. (33) to (38) govern the solution. After linearization we find the following equations for the static

configuration:

$$\frac{dF_0}{ds} = 0\,, \tag{39}$$
$$\frac{dG_0}{ds} = w\,, \tag{40}$$
$$\frac{dm_0}{ds} = F_0 \sin\theta_0 - G_0 \cos\theta_0\,, \tag{41}$$
$$\frac{d\theta_0}{ds} = m_0\,, \tag{42}$$
$$\frac{dx_0}{ds} = \cos\theta_0\,, \tag{43}$$
$$\frac{dy_0}{ds} = \sin\theta_0\,. \tag{44}$$

The procedure also results in the following equations for the first-order dynamics:

$$\frac{\partial F_1}{\partial s} = \frac{\partial^2 x_1}{\partial t^2}\,, \tag{45}$$
$$\frac{\partial G_1}{\partial s} = \frac{\partial^2 y_1}{\partial t^2}\,, \tag{46}$$
$$\frac{\partial m_1}{\partial s} = (F_0\theta_1 - G_1)\cos\theta_0 + (G_0\theta_1 + F_1)\sin\theta_0\,, \tag{47}$$
$$\frac{\partial \theta_1}{\partial s} = m_1\,, \tag{48}$$
$$\frac{\partial x_1}{\partial s} = -\theta_1 \sin\theta_0\,, \tag{49}$$
$$\frac{\partial y_1}{\partial s} = \theta_1 \cos\theta_0\,. \tag{50}$$

Equations (39) to (44) and Eqs. (45) to (50) are of course the same well-known sets of equations that govern small-on-large vibrations of fixed-length rods [8, 13].

3.3. Perturbation Expansion of Boundary Conditions

The appropriate boundary conditions at $s = 0$ are

$$\theta(0,t) = 0\,, \quad x(0,t) = 0\,, \quad y(0,t) = 1\,, \tag{51}$$

which are readily linearized to yield

$$\theta_0(0) = 0\,, \quad x_0(0) = 0\,, \quad y_0(0) = 1\,, \tag{52}$$

and

$$\theta_1(0,t) = 0\,, \quad x_1(0,t) = 0\,, \quad y_1(0,t) = 0\,. \tag{53}$$

Three relatively obvious boundary conditions at the contact point $s = \ell(t)$ are

$$m(\ell(t),t) = M_\ell\,, \quad \theta(\ell(t),t) = 0\,, \quad y(\ell(t),t) = 0\,. \tag{54}$$

Equations (51) and (54) altogether make up six boundary conditions, but seven are required to fully specify a solution. It is not immediately apparent what the seventh condition should be, but a hint is provided by the fact that there was no such confusion in Section 2. The essential effect that the foregoing approach neglects, but that is present in the small-on-large case, is horizontal momentum. Thus, it is likely that the missing condition should somehow involve $F(\ell(t),t)$, the axial force in the rod at the contact point.

Indeed, the segment $\ell(t) < s < L$ carries horizontal momentum as it slides left and right along the frictionless substrate, and this must be reflected in the force $F(\ell(t),t)$. A balance of linear momentum quickly yields

$$-F(\ell(t),t) = [L-\ell(t)]\frac{\partial^2 x}{\partial t^2}(\ell(t),t) - \dot{\ell}(t)\frac{\partial x}{\partial t}(\ell(t),t)\,, \tag{55}$$

which we emphasize is the elusive boundary condition in its dimensionless form. Notice that an additional parameter that was not present in the linear analysis has been introduced, namely the total length of the rod L.[4] There are two important limiting cases for this parameter: $L-\ell(t) \to 0^+$ and $L-\ell(t) \to \infty$. In the former, the rod contacts the substrate only over a very small region such that there is effectively zero axial force to first order acting at $s = \ell(t)$. In the latter, the inertia of the contacting segment is so large that it cannot accelerate along the substrate.

Writing the appropriate variables as regular perturbation series in ϵ, inserting them into Eqs. (54) and (55), expanding in Taylor series, and grouping like powers of ϵ, it is straightforward to show

$$F_0(\ell_0) = 0\,, \quad m_0(\ell_0) = M_\ell\,, \quad \theta_0(\ell_0) = 0\,, \quad y_0(\ell_0) = 0\,, \tag{56}$$

and

$$\underbrace{\frac{dF_0}{ds}(\ell_0)}_{=0 \text{ by Eq. (39)}}\ell_1(t) + F_1(\ell_0,t) + (L-\ell_0)\frac{\partial^2 x_1}{\partial t^2}(\ell_0,t) = 0\,, \tag{57}$$

$$\frac{dm_0}{ds}(\ell_0)\ell_1(t) + m_1(\ell_0,t) = 0\,, \tag{58}$$

$$\underbrace{\frac{d\theta_0}{ds}(\ell_0)}_{=M_\ell \text{ by Eqs. (42) and (56)}_2}\ell_1(t) + \theta_1(\ell_0,t) = 0\,, \tag{59}$$

$$\underbrace{\frac{dy_0}{ds}(\ell_0)}_{=0 \text{ by Eqs. (44) and (56)}_3}\ell_1(t) + y_1(\ell_0,t) = 0\,. \tag{60}$$

Combining Eqs. (58) and (59) in order to eliminate $\ell_1(t)$ results in a rotational spring boundary condition:

$$m_1(\ell_0,t) = K\theta_1(\ell_0,t), \quad K = \frac{1}{M_\ell}\frac{dm_0}{ds}(\ell_0)\,. \tag{61}$$

[4] We reiterate that physically meaningful solutions only exist when $\ell(t) < L$.

The spring constant K can be simplified somewhat by evaluating Eq. (41) at $s = \ell_0$ and taking into account Eq. $(56)_{1,3}$. Thus

$$K = -\frac{G_0(\ell_0)}{M_\ell}\,, \tag{62}$$

such that the stiffness of the spring is set by the ratio of the static shear force to the static bending moment at $s = \ell_0$.

To summarize, the boundary conditions for the dynamic variables at $s = \ell_0$ are

$$F_1(\ell_0, t) + (L - \ell_0)\frac{\partial^2 x_1}{\partial t^2}(\ell_0, t) = 0\,, \quad m_1(\ell_0, t) = K\theta_1(\ell_0, t)\,, \quad y_1(\ell_0, t) = 0\,, \tag{63}$$

with K as in Eq. (62). We now have six boundary conditions on the dynamic variables, the correct number required to specify a solution on $0 < s < \ell_0$. However, we have not used all of the information contained in Eqs. (57) to (60). In particular, we can use Eq. (58) to show

$$\ell_1(t) = \frac{m_1(\ell_0, t)}{G_0(\ell_0)}\,, \tag{64}$$

meaning that once the static and dynamic solutions are known, $\ell_1(t)$ can be computed with ease. It should be emphasized that $\ell_1(t)$ does not appear anywhere else in the equations that result from our solution procedure. Furthermore, in contrast to the small-on-small case discussed in Section 2.2, the boundary conditions at the contact point for the small-on-large analysis (i.e., Eq. (63)) do *not* in general represent a spatially fixed rotational spring but rather a rotational spring plus an attached mass that is free to slide horizontally.

3.4. Determination of Modes of Free Vibration

At this stage the static problem is fully defined by Eqs. (39) to (44) subject to Eq. (52) and Eq. (56). The dynamic problem is fully defined by Eqs. (45) to (50) subject to Eq. (53) and Eq. (63), and we seek solutions in which each of the *six* dynamic variables F_1, G_1, m_1, θ_1, x_1, and y_1 is separable into a mode shape and a sinusoid of angular frequency ω, e.g., $m_1(s, t) = \hat{m}_1(s)\cos(\omega t)$. Notice that, unlike previous work on similar problems (see [9, 11]), we make absolutely no assumption about the nature of $\ell_1(t)$, most certainly not the severe restriction that it too be sinusoidal with frequency ω.

It is easy to show from Eqs. (45) to (50) that the ordinary differential equations

governing the mode shape are

$$\frac{d\hat{F}_1}{ds} = -\omega^2 \hat{x}_1 \,, \tag{65}$$

$$\frac{d\hat{G}_1}{ds} = -\omega^2 \hat{y}_1 \,, \tag{66}$$

$$\frac{d\hat{m}_1}{ds} = (F_0\hat{\theta}_1 - \hat{G}_1)\cos\theta_0 + (G_0\hat{\theta}_1 + \hat{F}_1)\sin\theta_0 \,, \tag{67}$$

$$\frac{d\hat{\theta}_1}{ds} = \hat{m}_1 \,, \tag{68}$$

$$\frac{d\hat{x}_1}{ds} = -\hat{\theta}_1 \sin\theta_0 \,, \tag{69}$$

$$\frac{d\hat{y}_1}{ds} = \hat{\theta}_1 \cos\theta_0 \,. \tag{70}$$

The corresponding boundary conditions are likewise straightforward to obtain. Equation (53) promptly leads to

$$\hat{\theta}_1(0) = 0 \,, \quad \hat{x}_1(0) = 0 \,, \quad \hat{y}_1(0) = 0 \,, \tag{71}$$

while Eq. (63) yields

$$\hat{F}_1(\ell_0) = \omega^2(L - \ell_0)\hat{x}_1(\ell_0) \,, \quad \hat{m}_1(\ell_0) = K\hat{\theta}_1(\ell_0) \,, \quad \hat{y}_1(\ell_0) = 0 \,. \tag{72}$$

Equation $(72)_1$, which reflects a sort of spring with frequency-dependent stiffness, makes apparent two interesting limiting behaviors. For low-frequency oscillations ($\omega \to 0^+$), the point $s = \ell_0$ is connected to a rotational spring that is entirely free to move horizontally. By contrast, for high-frequency oscillations ($\omega \to \infty$), the point $s = \ell_0$ is connected to a spatially fixed rotational spring.

Once the static solution, mode shape, and natural frequency have been computed, one can calculate from Eq. (64) that

$$\ell_1(t) = \frac{\hat{m}_1(\ell_0)}{G_0(\ell_0)} \cos(\omega t) \,, \tag{73}$$

which shows that $m_1(s,t)$ being time-harmonic with angular frequency ω induces the same in $\ell_1(t)$. We emphasize that this was not assumed *a priori*.

3.5. Summary of Equations

To summarize, one must first solve Eqs. (39) to (44), subject to Eq. (52) and Eq. (56), for the static solution: the functions $F_0(s)$, $G_0(s)$, $m_0(s)$, $\theta_0(s)$, $x_0(s)$, and $y_0(s)$ on the interval $0 < s < \ell_0$, as well as the constant ℓ_0. Then, using said solution, one solves Eqs. (65) to (70), subject to Eqs. (71) and (72), for the mode shape defined by the functions $\hat{F}_1(s)$, $\hat{G}_1(s)$, $\hat{m}_1(s)$, $\hat{\theta}_1(s)$, $\hat{x}_1(s)$, and $\hat{y}_1(s)$ on the (now) fixed interval $0 < s < \ell_0$, as well as for the natural frequency ω. Thereafter $\ell_1(t)$ can be recovered according to Eq. (73) if so desired.

Just as in standard linear vibration analysis, the mode shape is only unique up to a scalar multiple; there are seven unknowns but just six boundary conditions. By

Eq. (73), the amplitude of the contact point oscillations is also indeterminate. For given values of the specific weight w, adhesive moment M_ℓ, and total length L, we use MATLAB's `bvp4c` solver to obtain numerical solutions of the standard boundary-eigenvalue problems for the static configuration, the mode shape, and the natural frequency. Because the amplitude of the mode shape is inherently indeterminate, it is necessary to specify an additional "fake" boundary condition that is independent of the others so as to ensure the numerical problem is not underdetermined.

4. Results

We now present the results of an extensive exploration of the parameter space of w, M_ℓ, and L. For the determination of the static configuration, we need not specify the total length L so long as we assume it is large enough that $L > \ell_0$, which we shall do. However, for the determination of the mode shapes and natural frequencies it is in fact necessary to specify a particular value of L. In order to limit the scope of our presentation to the convenient, two-dimensional parameter space (w, M_ℓ), we would like to take the limit $L \to \infty$, in which case we naively expect Eq. $(72)_1$ would degenerate to a boundary condition akin to a spatially fixed rotational spring. However, we will demonstrate shortly that said limit is in fact singular in the sense that, if we first take $L \to \infty$ and then take $w \to 0^+$ and $M_\ell \to 0^+$, we obtain natural frequencies that differ by a finite amount from the results of the small-on-small analysis, in which $w \to 0^+$ and $M_\ell \to 0^+$ are assumed at the outset. A related singular limit has been identified in analyzing the vibration of a fixed-length rod about its static configuration [8], so it is not too surprising that one appears here as well.

4.1. Static Equilibrium

We first study the simple correspondence between the static non-contacting length ℓ_0 and the parameters w and M_ℓ. (Recall that L does not affect the static equilibrium so long as we take it large enough that $L > \ell_0$.) Figure 3 depicts the parametric dependence of ℓ_0 in the gravity-only and adhesion-only cases. We see that the linear analysis of Section 2.3 provides a satisfactory approximation when $w \ll 1$ or $M_\ell \ll 1$, but at the same time $\ell_0 \to \infty$ as $w \to 0^+$ and $M_\ell \to 0^+$, a first sign that we might be facing a problem with a singular limit.

As in the beam-theoretic analysis of Section 2.3, there are only certain regions of the (w, M_ℓ)-plane that the rod can occupy. Perhaps surprisingly, solutions to the nonlinear problem appear only to exist, based purely on our numerical results, subject to the same condition obtained previously, i.e., $M_\ell^2 + 2w \geq 0$. The boundary between the gravity-dominant and adhesion-dominant regions, however, is different, as is easily seen in Fig. 4, which depicts the various regions in the plane and introduces a color scheme used in subsequent plots. It also shows how the static non-contacting length ℓ_0 varies according to w and M_ℓ. Notice that the boundary of the "no solution" region can be thought of as the contour corresponding to $\ell_0 \to \infty$.

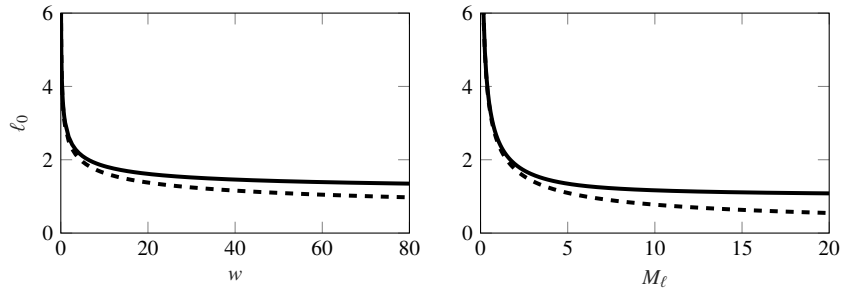

(a) Gravity only.

(b) Adhesion only.

Figure 3: Dependence of the static non-contacting length ℓ_0 on the weight per unit length w and adhesive moment M_ℓ when (a) $M_\ell = 0$ and (b) $w = 0$. The dashed lines correspond to the results from the Euler-Bernoulli analysis, Eq. (31), when $M_\ell = 0$ and $w = 0$, respectively.

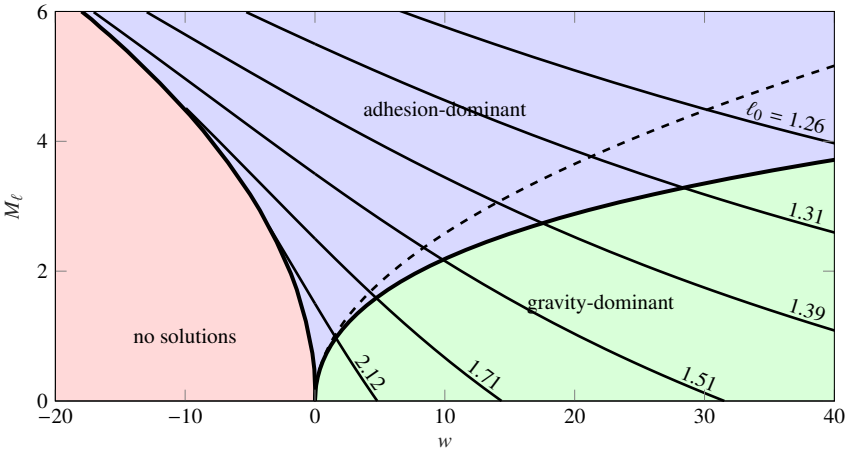

Figure 4: Classification of static solutions to the fully nonlinear problem according to the parameters w and M_ℓ and a sample of contours of constant non-contacting length ℓ_0. The dotted line is the boundary determined from the linear analysis of Section 2.3. The reader is referred to the online version of this article for the figure in full color.

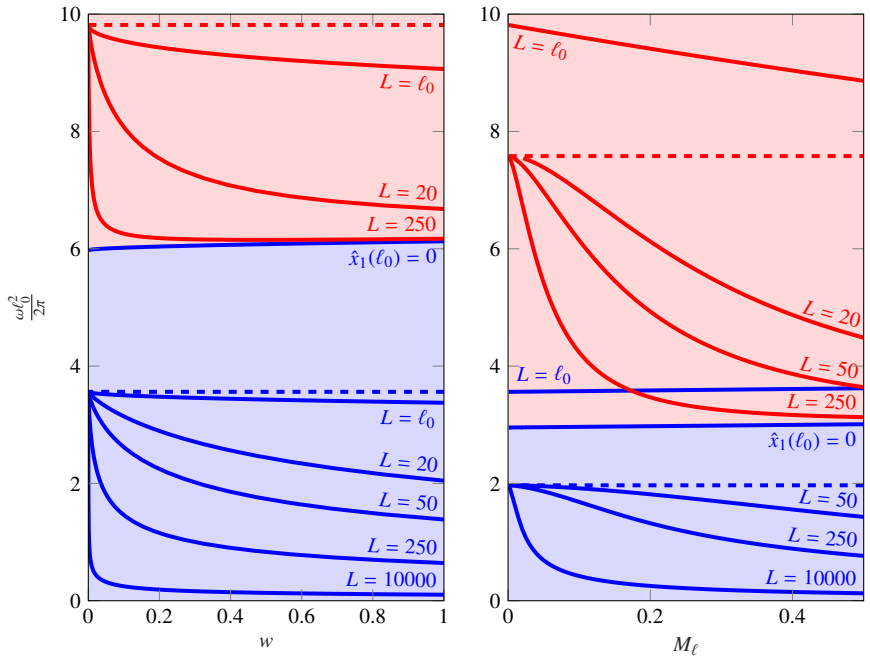

(a) Gravity only.

(b) Adhesion only.

Figure 5: Dependence of the first two natural frequencies on the weight per unit length w and adhesive moment M_ℓ when (a) $M_\ell = 0$ and (b) $w = 0$. The dashed lines correspond to the results for the Euler-Bernoulli beam, i.e. the first two roots of Eq. (6) and Eq. (A.10), respectively. The reader is referred to the online version of this article for the figure in full color. Blue curves indicate the first natural frequencies and red ones the second.

4.2. Mode Shapes and Natural Frequencies

As a first step in understanding the vibration behavior, we focus on the case where $w > 0$ and $M_\ell = 0$, remembering that the parameter L must be reintroduced. We are interested in examining the natural frequencies in the limit $w \to 0^+$ for various L, and determining how they relate to those obtained via the linear analysis presented in Section 2.3 and expounded upon in Appendix A.

Recall that $L = \ell_0$ corresponds to a rod whose tip is just barely touching the substrate and, by Eq. $(72)_1$, $\hat{F}_1(\ell_0) = 0$. For L very large, on the other hand, we expect (naively) that $\hat{x}_1(\ell_0) = 0$. With reference to Fig. 5a, observe that as L is increased, a boundary layer develops in the vicinity of $w = 0$ and, in the limit $L \to \infty$, the first natural frequency appears to tend toward zero for all w. However, if we take the boundary condition $\hat{x}_1(\ell_0) = 0$, then the first natural frequency for any given w is obviously not zero, but rather some finite value, hence the singular nature of the problem. Said finite value then serves as the lower bound for the *second* natural frequency for all L, again shown in Fig. 5a.

In a certain sense, the limit $L \to \infty$ causes the first mode to "disappear." Indeed, there is a marked qualitative difference in the mode shape when one takes as a boundary

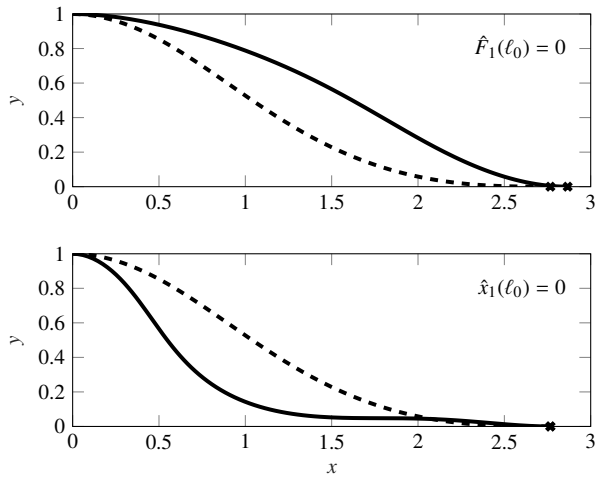

Figure 6: Comparison of typical shapes of the first mode of vibration with the distinct boundary conditions $\hat{F}_1(\ell_0) = 0$ and $\hat{x}_1(\ell_0) = 0$. We have taken $w = 1$ and $M_\ell = 0$. The dashed curves represent the static equilibrium and the point $s = \ell_0$ is marked with $\times$. See the Supplementary Material for an animation of the first, second, and third mode shapes.

condition Eq. $(72)_1$ with $\ell_0 \leq L < \infty$ as compared to when one replaces it by $\hat{x}_1(\ell_0) = 0$. As illustrated in Fig. 6, the mode shape has one inflection point and does not cross the static configuration in the former case, while it has two inflection points and *does* cross the static configuration in the latter. Additionally, the material point $s = \ell_0$ slides along the substrate in the former case while it remains stationary in the latter. A useful heuristic for understanding the singular limit is to envision the vibrating rod as a single-degree-of-freedom mass-spring system in which the contacting segment is the mass $m \propto L$ and the non-contacting segment is the spring with stiffness k. For a fixed k (i.e. fixed static configuration), the natural frequency $\sqrt{k/m}$ tends to zero as $m \to \infty$.

A similar behavior arises when $w = 0$ and $M_\ell > 0$. Referring to Fig. 5b, as L is increased, the first natural frequency tends to zero for all M_ℓ, and the first mode "disappears" in the same fashion as before. The adhesion-only case contrasts with its gravity-only counterpart in that the limit $L - \ell_0 \to 0^+$ is *also* singular. To be clear, this means that if one replaces Eq. $(72)_1$ with $\hat{F}_1(\ell_0) = 0$, the resulting natural frequencies differ by a finite amount and do not converge as $M_\ell \to 0^+$, a fact that the curves labeled $L = \ell_0$ in Fig. 5b clearly demonstrate.

Having highlighted the difficulties than can arise with limiting values of the parameter L, we now present some results in which both gravity and adhesion are considered, taking the boundary condition $\hat{x}_1(\ell_0) = 0$ for specificity. Figures 7a and 7b show a few contours of constant first and second natural frequency, respectively, in the (w, M_ℓ)-plane. In both instances the contours demonstrate a remarkable qualitative similarity. Focusing on Fig. 7a, the boundary between where solutions exist and where they do not appears to correspond to $\omega \to 0^+$. Normally such a behavior would be suggestive of a divergence instability, but in our case a more direct interpretation is possible. Figure 4 suggests that $\ell_0 \to \infty$ as one approaches the existence boundary such that the rod under

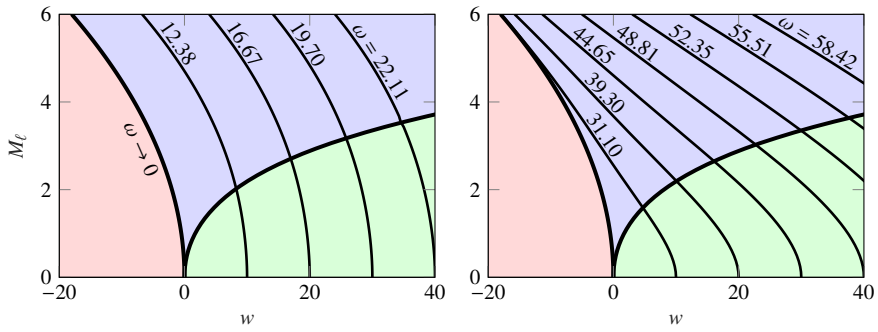

(a) First natural frequency.

(b) Second natural frequency.

Figure 7: First two natural frequencies as a function of w and M_ℓ. Contours of constant ω are indicated. See Fig. 4 for an interpretation of the colors.

consideration is one of semi-infinite length. The natural frequency tending to zero then reflects the well-known fact that a semi-infinite rod can sustain traveling waves.

4.3. Stability

All of the computed natural frequencies being real, the preceding linear vibration analysis shows the existence of (linearly) stable modes of vibration everywhere in the phase diagram that a static configuration exists. In other words, the system suffers neither a flutter- nor divergence-type instability. It is nevertheless instructive to apply what is known from the stability theory of elastic rods to the same problem.

An energy-based stability criterion for a statically deformed rod where one end is free to move on a rigid surface was recently formulated [20, 21]. The criterion, summarized in Appendix B, provides a necessary condition for the nonlinear stability of the system to small perturbations. Application of the criterion shows that configurations where $M_\ell \geq 0$ and $w > 0$ satisfy the necessary condition. However, configurations where $M_\ell \geq 0$ and $w < 0$ do not satisfy the criterion, thereby indicating an instability. However, this conclusion is at odds with the vibration-based analysis and we have been unable to resolve this discrepancy.

5. Conclusion

In this paper we have proposed a systematic method of analyzing small-amplitude vibrations about static equilibria of rods whose length is variable, inspired by several impressive contributions in the existing literature. The essence is to express each quantity as a perturbation series and to expand the boundary conditions in Taylor series about the material points that correspond to the boundaries of the static configuration. We have placed special emphasis on unilateral contact, and in particular on the industrially relevant problem of a heavy rod that is clamped at a certain height at one end and in adhesive contact with a flat, rigid surface at the other. In applying the perturbation method to this problem in both its "small-on-small" and "small-on-large" flavors, we have obtained several counterintuititve results.

It was shown in Section 2.2 that the seemingly mysterious correspondence between the natural frequencies of the aforementioned small-on-small system with zero adhesion and those of a fixed-fixed beam, as first observed by Roy and Chatterjee [11], is not so perplexing after all. Indeed, our method makes it clear that it is not just the natural frequencies that match those of a fixed-fixed beam, but rather the entire leading-order dynamics. When adhesion is included, as discussed in Section 2.3, the leading-order dynamics correspond to those of a beam that is clamped at one end and attached to a spatially fixed rotational spring at the other. (In fact, we showed the more general and apparently novel result that an adhesion boundary condition is equivalent to a spatially fixed rotational spring when the motion of the contact point is small.) Solutions only exist when the dimensionless specific weight w and adhesive moment M_ℓ satisfy a certain necessary condition that leads to a clear classification of solutions in the (w, M_ℓ)-plane.

Sections 3 and 4 concerned the application of the perturbation method to the corresponding small-on-large problem. A number of new phenomena arise, owing to the inclusion of horizontal momentum. It was shown that the *total* length of the rod L, not just the length ℓ_0 of the non-contacting segment, is a critical parameter in determining the natural frequencies. In fact, the limits $L \to \infty$ and $L - \ell_0 \to 0^+$ can both be singular. Numerical evidence suggests that solutions to the small-on-large problem only exist in the same region of the (w, M_ℓ)-plane as do solutions to the small-on-small problem, an unexpected result. Furthermore, the contour bounding the region where solutions do not exist appears to correspond to a curve of zero natural frequency.

Our results suggest numerous avenues for further research. An exploration of the nonlinear vibration effects that arise when terms are retained to $O(\epsilon^2)$ or higher is of interest [10, 23], as is a generalization of our approach to three dimensions. A particularly intriguing aspect of the problem studied in this paper is the nature of the boundary of the region of the (w, M_ℓ)-plane where no solutions exist, and we hope to see future work on why it is the same for the small-on-small and small-on-large problems, as well as how it relates to vibration, stability, and existence of static equilibria.

References

[1] L. Vu-Quoc and S. Li. Dynamics of sliding geometrically-exact beams: Large angle maneuver and parametric resonance. *Computer Methods in Applied Mechanics and Engineering*, 120(1-2):65–118, January 1995.

[2] Nikhil Singh, Ishan Sharma, and Shakti Singh Gupta. Dynamics of Variable Length Geometrically Exact Beams in Three-Dimensions. *International Journal of Solids and Structures*, page S0020768319304664, November 2019.

[3] L. Mansfield and J. G. Simmonds. The Reverse Spaghetti Problem: Drooping Motion of an Elastica Issuing from a Horizontal Guide. *Journal of Applied Mechanics*, 54(1):147, 1987.

[4] Dominic Vella, Arezki Boudaoud, and Mokhtar Adda-Bedia. Statics and Inertial Dynamics of a Ruck in a Rug. *Physical Review Letters*, 103(17):174301, October 2009.

[5] G. Napoli and A. Goriely. A tale of two nested elastic rings. *Proceedings of the Royal Society A: Mathematical, Physical and Engineering Sciences*, 473(2204):20170340, August 2017.

[6] Nathaniel N. Goldberg and Oliver M. O'Reilly. Mechanics-based model for the cooking-induced deformation of spaghetti. *Physical Review E*, 101(1):013001, January 2020.

[7] C. Y. Wang. Lifting of Heavy Elastic Sheet. *Journal of Engineering Mechanics*, 109(1):47–53, February 1983.

[8] Sébastien Neukirch, Joël Frelat, Alain Goriely, and Corrado Maurini. Vibrations of post-buckled rods: The singular inextensible limit. *Journal of Sound and Vibration*, 331(3):704–720, January 2012.

[9] Lucio Demeio and Stefano Lenci. Forced nonlinear oscillations of semi-infinite cables and beams resting on a unilateral elastic substrate. *Nonlinear Dynamics*, 49(1-2):203–215, May 2007.

[10] Ioannis K. Chatjigeorgiou. Second-order nonlinear dynamics of catenary pipelines: A frequency domain approach. *Computers & Structures*, 123:1–14, July 2013.

[11] Arjun Roy and Anindya Chatterjee. Vibrations of a Beam in Variable Contact With a Flat Surface. *Journal of Vibration and Acoustics*, 131(4):041010, August 2009.

[12] Yury Vetyukov, Evgenii Oborin, Jakob Scheidl, Michael Krommer, and Christian Schmidrathner. Flexible belt hanging on two pulleys: Contact problem at non-material kinematic description. *International Journal of Solids and Structures*, 168:183–193, August 2019.

[13] Raymond H. Plaut and Lawrence N. Virgin. Deformation and vibration of upright loops on a foundation and of hanging loops. *International Journal of Solids and Structures*, 51(18):3067–3075, September 2014.

[14] Lawrence N. Virgin, Joe V. Giliberto, and Raymond H. Plaut. Deformation and vibration of compressed, nested, elastic rings on rigid base. *Thin-Walled Structures*, 132:167–175, November 2018.

[15] A. Humer and H. Irschik. Large deformation and stability of an extensible elastica with an unknown length. *International Journal of Solids and Structures*, 48(9):1301–1310, May 2011.

[16] Lucio Demeio and Stefano Lenci. Second-order solutions for the dynamics of a semi-infinite cable on a unilateral substrate. *Journal of Sound and Vibration*, 315(3):414–432, August 2008.

[17] Wei-Chia Ro, Jen-San Chen, and Shau-Yu Hong. Vibration and stability of a constrained elastica with variable length. *International Journal of Solids and Structures*, 47(16):2143–2154, August 2010.

[18] S. Chucheepsakul and T. Monprapussorn. Divergence instability of variable-arc-length elastica pipes transporting fluid. *Journal of Fluids and Structures*, 14(6):895–916, August 2000.

[19] Costanza Armanini, Francesco Dal Corso, Diego Misseroni, and Davide Bigoni. Configurational forces and nonlinear structural dynamics. *Journal of the Mechanics and Physics of Solids*, 130:82–100, September 2019.

[20] C. Majidi, O. M. O'Reilly, and J. A. Williams. On the stability of a rod adhering to a rigid surface: Shear-induced stable adhesion and the instability of peeling. *Journal of the Mechanics and Physics of Solids*, 60(5):827–843, 2012.

[21] C. Majidi, O. M. O'Reilly, and J. A. Williams. Bifurcations and instability in the adhesion of intrinsically curved rods. *Mechanics Research Communications*, 49(0):13–16, 2013.

[22] O. M. O'Reilly. *Modeling Nonlinear Problems in the Mechanics of Strings and Rods: The Role of the Balance Laws*. Interaction of Mechanics and Mathematics. Springer, 2017.

[23] Lucio Demeio, Giovanni Lancioni, and Stefano Lenci. Nonlinear resonances in infinitely long 1D continua on a tensionless substrate. *Nonlinear Dynamics*, 66(3):271–284, November 2011.

Appendix A. Small-on-Small Vibrations with Combined Gravity and Adhesion

Recall that the leading-order dynamics of the linearized system are governed by Eqs. (21) to (24) and Eq. (29), except with the rotational spring stiffness K given by Eq. (32). Following the standard procedure, we seek solutions of the form $y_1(x,t) = Y(x)\sin(\omega t)$ with the goal of determining the admissible natural frequencies ω. We then must solve

$$-\omega^2 Y + \frac{d^4Y}{dx^4} = 0 \tag{A.1}$$

subject to

$$Y(0) = 0\,, \quad \frac{dY}{dx}(0) = 0\,, \quad Y(\ell_0) = 0\,, \quad \frac{d^2Y}{dx^2}(\ell_0) = K\frac{dY}{dx}(\ell_0)\,. \tag{A.2}$$

Introducing $\beta = \sqrt{\omega}$, the general solution of Eq. (A.1) is

$$Y(x) = A\cos(\beta x) + B\sin(\beta x) + C\cosh(\beta x) + D\sinh(\beta x)\,. \tag{A.3}$$

Applying Eq. $(A.2)_{1,2}$ leads to

$$Y(x) = A[\cos(\beta x) - \cosh(\beta x)] + B[\sin(\beta x) - \sinh(\beta x)]\,. \tag{A.4}$$

Equation $(A.2)_{3,4}$ give rise to an algebraic system of the form

$$\begin{bmatrix} c_1 & c_2 \\ c_3 & c_4 \end{bmatrix}\begin{bmatrix} A \\ B \end{bmatrix} = \begin{bmatrix} 0 \\ 0 \end{bmatrix}, \tag{A.5}$$

where

$$c_1(\beta; w, M_\ell) = K[\sin(\beta\ell_0) + \sinh(\beta\ell_0)] - \beta[\cos(\beta\ell_0) + \cosh(\beta\ell_0)]\,, \tag{A.6}$$

$$c_2(\beta; w, M_\ell) = -K[\cos(\beta\ell_0) - \cosh(\beta\ell_0)] - \beta[\sin(\beta\ell_0) + \sinh(\beta\ell_0)]\,, \tag{A.7}$$

$$c_3(\beta; w, M_\ell) = \cos(\beta\ell_0) - \cosh(\beta\ell_0)\,, \tag{A.8}$$

$$c_4(\beta; w, M_\ell) = \sin(\beta\ell_0) - \sinh(\beta\ell_0)\,. \tag{A.9}$$

In order for non-trivial solutions of Eq. (A.5) to exist, we must have

$$c_1 c_4 - c_2 c_3 = 0\,. \tag{A.10}$$

Given the parameters w and M_ℓ as well as ℓ_0 from the corresponding static solution, Eq. (A.10) is a transcendental equation for $\beta = \sqrt{\omega}$ that is readily solved with a numerical root-finding method.

Appendix B. Nonlinear Stability

For completeness, we present a nonlinear stability criterion for the static equilibrium configuration of a heavy elastic rod with one end fixed and the other end contacting a smooth surface with the possible presence of dry adhesion. The criterion was developed by Majidi et al. [20, 21] and is based on establishing conditions by which the potential energy functional is minimized with respect to perturbations in $\theta_0(s)$ and ℓ_0 that preserve the boundary conditions. The version of the criterion for the problem of interest here is discussed by O'Reilly [22, Section 4.7.2].

For a given static configuration of the rod, $\theta_0(s)$ and ℓ_0 are known. There are two parts to the criterion. The first part verifies that the rod has not buckled by finding a bounded solution $r(s)$ to a Ricatti equation:

$$\frac{dr}{ds} + P_0 - \frac{r^2}{EI} = 0\,, \qquad r(0) = 0\,, \qquad s \in [0, \ell_0)\,, \tag{B.1}$$

where $P_0 = P_0(s)$ is the tangential component of the contact force (or tension) in the rod:

$$P_0 = F_0 \cos\theta_0 + G_0 \sin\theta_0\,. \tag{B.2}$$

The second part captures stability with respect to perturbations to ℓ_0:

$$S_0 \frac{d\theta_0}{ds}(\ell_0^-) - \rho_0 g \sin\theta_0(\ell_0^-) \geq \left[\frac{d\theta_0}{ds}\left(\ell_0^-\right)\right]^2 r(\ell_0^-)\,, \tag{B.3}$$

where

$$S_0 = -EI\frac{d^2\theta_0}{ds^2}(\ell_0^-)\,, \tag{B.4}$$

and, for any function $f(x)$,

$$f(\ell_0^-) = \lim_{\sigma\to 0} f(\ell_0 - \sigma)\,, \qquad \sigma > 0\,. \tag{B.5}$$

For a given static configuration of the rod, if a bounded solution $r = r(s)$ to Eq. (B.1) can be found and Eq. (B.3) is satisfied, then the static configuration is said to be nonlinearly stable.

For the problem at hand $\theta_0(\ell_0) = 0$ and we can use Eq. (41) to simplify the expression for S_0: $S_0 = G_0$. Thus, Eq. (B.3) simplifies to

$$G_0 \geq \left[\frac{d\theta_0}{ds}(\ell_0^-)\right] r(\ell_0^-). \tag{B.6}$$

While G_0 is the vertical component of the contact force in the rod, the inequality Eq. (B.6) has no obvious physical interpretation.